RAPID COMMUNICATIONS

Single-crystal elasticity of MgO at high pressure

S. V. Sinogeikin and J. D. Bass

Department of Geology, University of Illinois at Urbana-Champaign, Urbana, Illinois 61801

(Received 29 December 1998)

The single-crystal elastic properties of MgO were measured by Brillouin scattering in diamond anvil cell to 18.6 GPa. These measurements demonstrate that quasihydrostatic stress conditions can be obtained in solid pressure medium by thermal annealing, and establish the accuracy with which elastic moduli can be measured over this extensive pressure range ($\pm5\%$ in dC_{ij}/dP). The acoustic anisotropy of MgO decreases with pressure, with MgO becoming isotropic at ~21.5 GPa. Deviations from noncentral interatomic forces, as measured by the Cauchy relations, increase steadily with pressure. [S0163-1829(99)50222-1]

Magnesium oxide has long been of interest as a prototype for understanding bonding in alkaline-earth oxides, as a commercially important ceramic, and as a likely major constituent of the Earth's lower mantle (between 660 km and 2900 km in depth).[1] The extensive literature on MgO includes both theoretical and experimental studies of its electronic structure,[2] structural phase transitions,[2–4] elasticity,[3–7] and thermal properties.[8] Because MgO is likely to be a major constituent of the Earth's lower mantle, the effects of pressure on bonding in MgO, and its properties under the high-pressure conditions, are of considerable importance to geophysics.[1–7,9–11] The long history of intense research on MgO also makes it useful as an interlaboratory standard for assessing the accuracy of new experimental techniques[6,10] and theoretical models.[4]

Here we present measurements of the single-crystal elastic properties of MgO to 18.6 GPa by Brillouin scattering in the diamond-anvil cell at room temperature. We used a Merrill-Bassett type four-screw diamond anvil cell (DAC) which was modified with a large opening for either 80° or 90° Brillouin scattering experiments.[12] Diamonds with culet diameters of 500 μm were used with gaskets of either 250 μm thick spring steel foil, or rhenium when annealing was necessary. Thin slabs (10–50 μm thick) were cut perpendicular to the [100] crystallographic direction from a single crystal of synthetic MgO (Ref. 7) and polished on both sides. Samples with dimensions of $\sim80\times80$ to 150×150 μm were cleaved from these slabs and loaded into the sample chamber
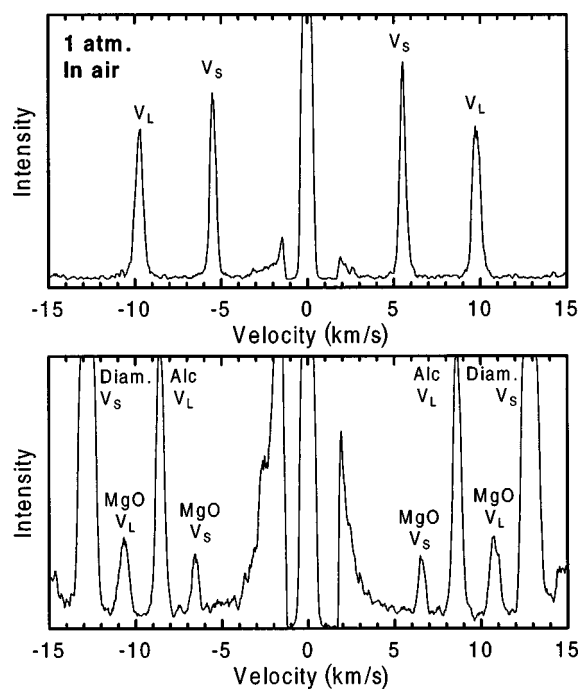

FIG. 1. Brillouin spectrum of MgO at 1 atm (top) and in DAC at 18.6 GPa (bottom). Longitudinal and shear peaks for MgO, longitudinal peaks for the methanol-ethanol-water mixture (Alc V_L), and shear peaks for diamonds (Diam. V_S) are also present.
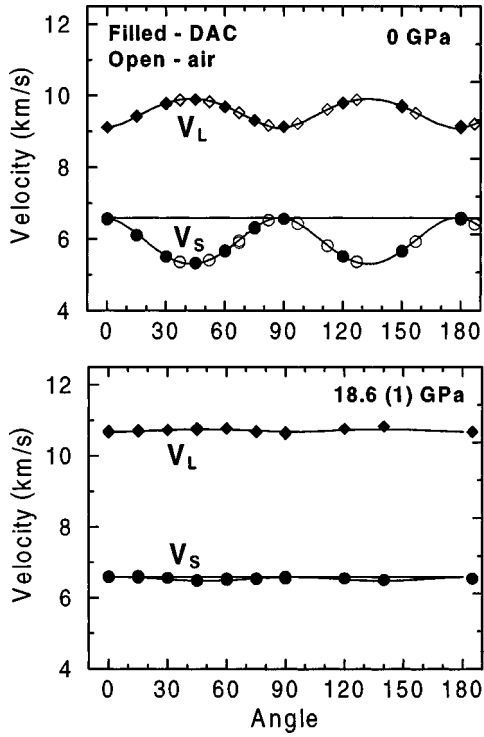
FIG. 2. Acoustic velocities as a function of phonon direction in the (100) plane at 1 atm (top) and at 18.6 GPa (bottom). Date obtained in air without the DAC (open symbols) are internally consistent with experiments in the DAC (filled symbols) at 1 atm. Decreased anisotropy is apparent in the data at 18.6 GPa.

along with typically 5–7 ruby chips for measurements of pressure, pressure gradients, and nonhydrostaticity. The pressure was calculated from the ruby fluorescence $R1$ line shift.[13,14] The pressure was measured before and after each experiment.

For Brillouin scattering we used an Argon ion laser ($\lambda_0 = 514.5$ nm) and a 6-pass tandem Fabry-Pérot interferometer. Details of the Brillouin spectrometer are given in Ref. 15. All experiments used a platelet/symmetric scattering geometry[12] with a scattering angle of 80°. The Brillouin spectra collected at $P = 1$ atm and at high pressure were of superb quality, with a very high signal-to-noise ratio (Fig. 1). To verify the reliability of the high-pressure results, we collected 1 atm data from an MgO platelet in air without the DAC, and also from a sample inside of the diamond cell at $P = 1$ atm (as indicated by the presence of an air bubble). The phonon velocities as a function of crystallographic direction are shown on Fig. 2, and show complete internal consistency between the data obtained with and without the DAC. This is strong evidence that our diamond cell results are accurate, and that we have avoided errors caused by strong refraction from the diamonds, and vignetting of the input/scattered light. We note that in order to obtain accurate Brillouin results at high pressures, it is important that the sample and diamond surfaces be strictly parallel throughout the experiment, that the scattering geometry by carefully controlled, and that the gasket hole used as a sample chamber not intercept any part of the incident or scattered cones of light.

High-pressure data were collected at hydrostatic pressures of 2.5(1), 5.5(1), 7.9(1), 11.0(1), 14.4(3), 14.6(3), and 18.6(2) GPa. The numbers in parentheses are the estimated
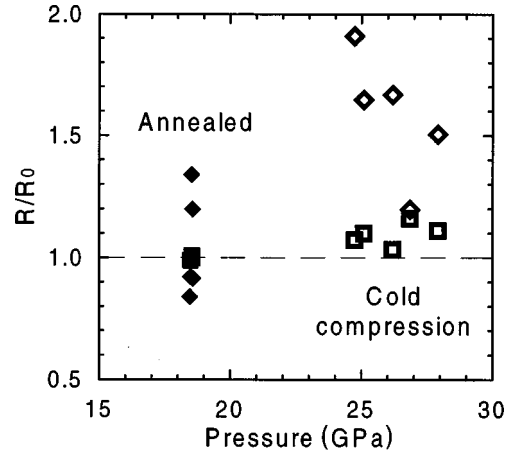

FIG. 3. Ruby peak widths, $R1$-$R2$ peak splitting, and pressure gradients in the diamond cell before and after annealing. Diamonds indicate the width of ruby $R1$ fluorescence peaks normalized to 1-atm value. Squares indicate the normalized $R1$-$R2$ peak splitting. Note the range in pressure values (~3 GPa) before annealing, and very consistent pressure values after annealing.

1σ uncertainties in pressure measurement, calculated from the run-to-run variation of fluorescence measurements, but do not include possible systematic errors in the ruby pressure scale. A mixture of methanol, ethanol, and water (16:3:1 by volume) was used as a pressure-transmitting medium in all experiments. This fluid has a freezing pressure at room temperature of ~15 GPa, and we observed that the ruby fluorescence peaks remained sharp and narrow up to that pressure.

Even at pressures above the freezing point of the pressure medium, a near hydrostatic stress state can be achieved in the DAC by thermal annealing. In all runs above 10 GPa the

TABLE I. Single-crystal and aggregate elastic moduli of MgO (in GPa) and their pressure derivatives. Pressure derivatives of bulk and shear moduli are calculated from finite-strain equations of state. Pressure derivates of single-crystal elastic constants are given polynomial fits: $C_{ij}(P) = C_{ij_0} + C'_{ij}P + \frac{1}{2}C''_{ij}P^2$. In Ref. 10 two sets of pressure derivatives are presented, both of which we list.

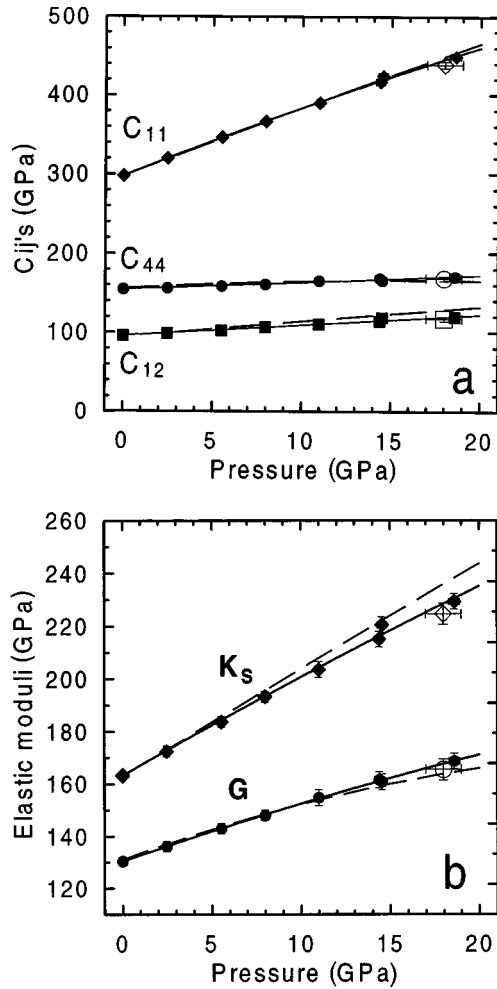| Modulus	This study	Ref. 9, to 3 GPa	Ref. 10, to 7.8 GPa
C_{11}	297.9(15)	296.8(2)	297.8
C'_{11}	9.05(20)	9.17(7)	8.76/8.75
C''_{11}	−0.090(30)	−0.118(60)	−0.030/−0.038
C_{44}	154.4(20)	155.8(2)	155.8(15)
C'_{44}	0.84(20)	1.11(1)	1.31/1.29
C''_{44}	+0.006(20)	−0.032(6)	−0.09/−0.075
C_{12}	95.8(10)	95.3(2)	95.1
C'_{12}	1.34(15)	1.61(12)	1.81/1.99
C''_{12}	−0.002(20)	−0.028(68)	0.02/−0.026
K_0	163.2(10)	162.5(2)	162.7(2)
K'_0	4.0(1)	4.13(9)	4.13/4.24
K''_0	−0.04(2)	−0.058(66)	0.001/−0.029
G_0	130.2(10)		
G'_0	2.4(1)		
G''_0	−0.04(2)		

FIG. 4. Single-crystal elastic moduli of MgO (a), and isotropic aggregate bulk and shear moduli (b) as a function of pressure. Open symbols indicate results for a nonhydrostatic experiment. Solid lines are polynomial fits (a), or finite strain fits (b), to our data. Extrapolations of data from Ref. 9 are indistinguishable from the solid curves. Dashed lines are extrapolations of data from Ref. 10.

diamond cell was heated to 150–200 °C for 10–60 min, with longer anneals at higher pressures. The hydrostaticity of the pressure-transmitting medium can be estimated from pressure gradients inside the diamond cell, the splitting of $R1$-$R2$ ruby peaks, and the width of the ruby peaks.[16–18] In Fig. 3 the ruby linewidths and $R1$-$R2$ peak splitting are shown for different ruby chips in a single run, both before and after heat treatment. While there is a small variability in the linewidth (which can be partially due to the instrumental function), both the pressure gradient and increased line splitting are eliminated during heating, indicating that annealing produces essentially hydrostatic conditions within the resolution of our experiments.

From the measured Brillouin spectra, acoustic velocities are obtained through the relation

$$V_i = \tfrac{1}{2} \Delta \omega_i \lambda_0 / \sin(\theta/2),$$

where V_i is a phonon velocity, $\Delta \omega_i$ is the measured Brillouin shift, λ_0 is the laser wavelength, and θ is the angle between the incident and scattered light measured outside the DAC.[12]
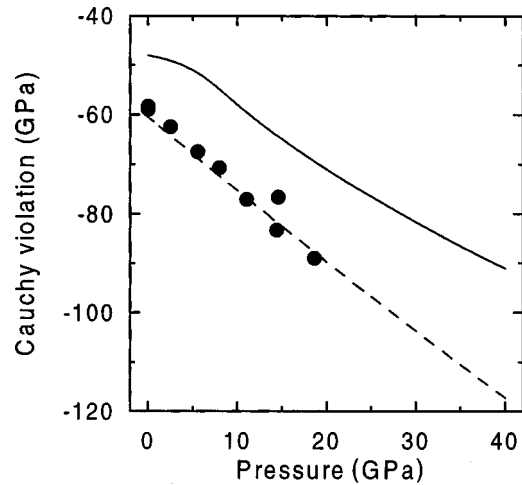

FIG. 5. Deviations from the Cauchy relation as a function of pressure. Solid symbols are from this study. The solid line is the calculated result of Ref. 5. The dashed line is an extrapolation of results from Ref. 9.

In the symmetric platelet scattering geometry, velocities are determined independent of the refractive index of the sample.

MgO is cubic and characterized by three independent elastic moduli. All three moduli can be deduced from velocity measurements in any crystallographic plane. Use of the Merrill-Bassett cell and platelet/symmetric geometry allowed us to measure velocities for any phonon direction within the plane of the platelet [the (100) crystallographic plane]. Typically we collected Brillouin spectra in ten directions over a 180° angle within (100).

Phonon velocities are related to the single-crystal elastic moduli through the Christoffel equation:[19]

$$\det \left| C_{ijkl} n_j n_l - \rho V^2 \delta_{ik} \right| = 0,$$

where C_{ijkl} is the elastic modulus tensor, n_j and n_l are the direction cosines of the phonon, ρ is the density, V is the phonon velocity, and δ_{ik} is the Kronecker delta. Throughout the rest of this paper the elastic moduli are indicated by the reduced Voigt notation C_{ij}. We used a linearized inversion procedure to solve for the three independent elastic moduli, C_{ij}, at each pressure. Because the C_{ij} and the density are interdependent, an iterative procedure was used to obtain the density, C_{ij}'s, and isotropic aggregate elastic moduli using a fourth-order finite strain equation of state (EOS).[20] This procedure is insensitive to the initial estimates used in the regression and rapidly converges to stable values for the aggregate elastic moduli K (the bulk modulus), G (the shear modulus), and their pressure derivatives. We then use polynomials to represent the pressure dependence of the C_{ij}'s reported in Table I.

Our results for the single-crystal elastic moduli and isotropic aggregate moduli (K and G) are in excellent agreement with a finite-strain extrapolation of the date of Jackson and Niesler[9] measured to hydrostatic pressures of 3 GPa (Fig. 4, Table I). In contrast, our results are only marginally compatible with the nonhydrostatic results of Yoneda,[10] indicating that nonhydrostatic conditions significantly affect elastic property measurements. Although C_{11} and C_{44} from this

study and Ref. 10 agree to $P = 7.8$ GPa, the pressure derivative of the off-diagonal modulus C_{12} from the ultrasonic experiments of Ref. 10 is greater than our result. As a consequence, the bulk modulus is too large and the shear modulus is too low [Fig. 4(b)]. The discrepancy between our results and those of Yoneda[10] may be explained by a stiffening of the indium bond between the buffer rod and sample in their experiments, which causes shear stresses on the sample. This interpretation is supported by the agreement of our results with those of Ref. 9, and indicates that high-quality elasticity data collected under hydrostatic conditions can be accurately extrapolated to pressures well beyond the experimental range using a finite strain formalism. This conclusion differs from earlier studies which suggested that finite strain extrapolations to high pressure are unreliable.

One experiment was conducted under nonhydrostatic conditions to evaluate the effect of nonhydrostaticity on acoustic velocities and the elastic moduli. A 10 μm thick sample was loaded into the DAC at a pressure of $\sim$18(1) GPa without heat treatment of the pressure-transmitting medium. The pressure gradient in the cell was approximately 1.6 GPa. The ruby $R1$ line was $\sim$1.7 times wider than the linewidth at 1 atm. Both compressional and shear aggregate acoustic velocities were 0.7% lower than the trend defined by hydrostatic measurements. The single-crystal elastic moduli were therefore 1.2–2.0 % below the hydrostats [Fig. 4(a)]. Note that the average pressure in the nonhydrostatic experiment exceeds the freezing point of the pressure-transmitting medium by only $\sim$3 GPa. Because nonhydrostaticity increases rapidly with pressure, much higher stress gradients and systematic errors are expected at higher pressures. The first pressure derivatives of elastic moduli will be less affected by nonhydrostaticity, because they are determined primarily by the measurements at lower (presumably hydrostatic) pressures. However, the second pressure derivatives of single-crystal, bulk, and shear moduli will be biased toward higher absolute values than those derived from hydrostatic experiments, leading to large uncertainties in extrapolations outside the experimental pressure range.

A knowledge of the acoustic anisotropy of minerals at high pressure impacts our interpretation of seismic wave anisotropy in the Earth's mantle, and puts constraints on our understanding of mantle composition. For cubic crystals, the ratio of $2C_{44}(C_{11} - C_{12})$ is a measure of elastic anisotropy, being equal to unity for an elastically isotropic material. The elastic anisotropy $A = (2C_{44} + C_{12})/C_{11} - 1$ is therefore zero for an isotropic material.[4] The anisotropy factor of MgO decreases from 0.36 at ambient pressure to 0.03 at 18.6 GPa. A short extrapolation indicates that MgO is elastically isotropic at 21.5 (10) GPa. At higher pressures the anisotropy increases with increasing pressure, although the sign of A is opposite that at $P < 21.5$ GPa.

The high-pressure Cauchy relation for hydrostatic conditions, $C_{12} - C_{44} = 2P$ (for crystals with cubic symmetry), will be satisfied when interatomic forces are purely central.[2,4,5,21] Figure 5 shows the deviations from the Cauchy condition measured in this study, and these results indicate the presence of highly noncentral forces in MgO. Moreover, deviations from the Cauchy relation increase (that is, become more negative) with increasing pressure, indicating that the noncentral nature of the bonding becomes greater at high pressures. These results provide direct experimental verification of recent first-principles calculations of elastic moduli in MgO (Ref. 4) which are also shown in Fig. 5 for comparison. The differences between the experimental and calculated values of the Cauchy violation are due primarily to C_{44} being underestimated in the calculations. This modulus is particularly sensitive to the type of pseudopotential used in the calculations.

[1] D. L. Anderson, *Theory of the Earth* (Blackwell Scientific, Boston, 1989).

[2] M. J. Mehl, R. E. Cohen, and H. Krakauer, J. Geophys. Res. **93**, 8009 (1988); A. J. Cohen and R. G. Gordon, Phys. Rev. B **14**, 4593 (1976).

[3] K. J. Chang and M. L. Cohen, Phys. Rev. B **30**, 4774 (1984).

[4] B. B. Karki *et al.*, Am. Mineral. **82**, 51 (1997).

[5] G. H. Wolf and M. S. T. Bukowinski, Phys. Chem. Miner. **15**, 209 (1988); D. G. Isaak, R. E. Cohen, and M. J. Mehl, J. Geophys. Res. **95**, 7055 (1990).

[6] G. Chen, R. C. Liebermann, and D. J. Weidner, Science **280**, 1913 (1998); H. Spetzler, J. Geophys. Res. **75**, 2073 (1970).

[7] T. S. Duffy and T. J. Ahrens, J. Geophys. Res. **100**, 529 (1995).

[8] I. Inbar and R. E. Cohen, Geophys. Res. Lett. **22**, 1533 (1995).

[9] I. Jackson and H. Niesler, in *High Pressure Research in Geophysics*, edited by S. Akimoto and M. H. Manghnani (Center for Academic Publications Japan, Tokyo, 1982), p. 93.

[10] A. Yoneda, J. Phys. Earth **38**, 19 (1990).

[11] T. S. Duffy, R. J. Hemley, and H.-K. Mao, Phys. Rev. Lett. **74**, 1371 (1995).

[12] C. H. Whitfield, E. M. Brody, and W. A. Bassett, Rev. Sci. Instrum. **47**, 942 (1976).

[13] H. K. Mao *et al.*, J. Appl. Phys. **49**, 3276 (1978).

[14] V. E. Bean *et al.*, Physica B **139&140**, 52 (1986).

[15] S. V. Sinogeikin, T. Katsura, and J. D. Bass, J. Geophys. Res. **103**, 20 819 (1998).

[16] X. A. Shen and Y. M. Gupta, Phys. Rev. B **48**, 2929 (1993).

[17] Y. M. Gupta, P. D. Horn, and J. A. Burt, J. Appl. Phys. **76**, 1784 (1994).

[18] S. M. Sharma and Y. M. Gupta, Phys. Rev. B **43**, 879 (1991).

[19] M. J. P. Musgrave, *Crystal Acoustics* (Holden-Day, San Francisco, 1970).

[20] G. F. Davies and A. M. Dziewonski, Phys. Earth Planet. Inter. **10**, 336 (1975).

[21] V. V. Brazhkin and A. G. Lyapin, Phys. Rev. Lett. **78**, 2493 (1997).